ELSEVIER

Surface Science 324 (1995) 91–105

surface science

Formation of two-dimensional sulfide phases on Al(111): an STM study

T. Wiederholt [a], H. Brune [a], J. Wintterlin [a,*], R.J. Behm [b], G. Ertl [a]

[a] *Fritz-Haber-Institut der Max-Planck-Gesellschaft, Faradayweg 4–6, D-14195 Berlin, Germany*
[b] *Abteilung Oberflächenchemie und Katalyse, Universität Ulm, D-89069 Ulm, Germany*

Received 8 August 1994; accepted for publication 1 November 1994

Abstract

The structure and growth of incommensurate phases, formed by dissociation of H_2S on Al(111) at 350 or 570 K, were studied by scanning tunneling microscopy. Various hexagonal structures were found, with lattice constants decreasing from 3.55 to 3.47 Å and rotational angles increasing from 0° to 8° with respect to the [1$\bar{1}$0] direction of the substrate. This points to rotational epitaxy, indicative of a flat interaction potential in relation to strong interactions within the adlayer. The exact structure of this phase varies slightly across the surface, local variations are introduced by edge dislocations or other defects. The adlayer nucleates at steps, after which triangular islands with very stable edges grow on the terraces. The initial nuclei are distinctly different from the islands, appearing much higher in the STM images. Larger coverages initiate restructuring and facetting of the Al substrate, indicating mass transport during formation of the adlayer. Our observations provide strong evidence for a composite, sulfide-like structure with strong internal interactions which involves a reconstruction of the substrate. The misfit of this hexagonal multilayer structure and the substrate leads to the moiré pattern observed by STM. The relatively flat interaction potential of this composite adlayer with the substrate allows various rotational orientations, depending on the exact, local coverage and adlayer lattice parameters.

Keywords: Aluminum; Chalcogens; Chemisorption; Compound formation; Low index single crystal surfaces; Scanning tunneling microscopy; Sulfides

1. Introduction

Sulfur adsorption on close-packed metal surfaces very often leads to relatively simple, $(n \times n)$ or $(\sqrt{n} \times \sqrt{n})$ structures, where the n are small integer numbers. Examples are the (2×2) structures on the (111) surfaces of Ni [1], Pt [2] and the $(\sqrt{3} \times \sqrt{3})R30°$ structures on Rh [3], Ir [4], Pd [5], and Pt [2]. More complicated structures, such as the $(5\sqrt{3} \times 2)$ structure on Ni(111) [6] are found in some cases at higher coverages, or when reconstructions are involved. However, the general prevailance of lattice-gas structures indicates a relatively large corrugation of the sulfur–metal interaction potential by which high-symmetry adsorption sites are favored.

A striking exception to this rule is sulfur adsorbed on the Al(111) surface. In a study using LEED (low energy electron diffraction) and ARUPS (angular resolved ultraviolet photoemission spectroscopy) Jacobi, Muschwitz, and Kambe [7] found that sulfur forms a hexagonal overlayer on Al(111), with lattice

* Corresponding author.

0039-6028/95/$09.50
SSDI 0039-6028(94)00732-2

vectors parallel to those of the substrate, but from the lattice constant of 3.5 Å no simple structure is compatible with the 2.86 Å of the aluminum substrate. It was therefore concluded that the structure is incommensurate. Incommensurate overlayer structures are well known from other systems, e.g., from physisorbed layers of noble gases [8–11], adsorbed alkali metals [11,12], and from some metal-on-metal systems [13]. A common feature of all of these cases is that the adsorbate–substrate potential is flat when compared to the magnitude of the adsorbate–adsorbate interactions, either because the adsorption energy as a whole is small (for the noble gases) or because the bonds to the surface are only little directional (for the alkali metals and the metal films). Consequently, since the sulfur–aluminum bond is strong (for S on the fcc sites on Al(111) an adsorption energy of 3.5 eV has been calculated [14]), and since the bond to the substrate should be covalent and directional (probably less so than for the above mentioned transition metals), the sulfur–sulfur interactions must be unusually large to overcome the effect of the substrate. In fact, there is evidence that such strong interactions between neighboring S atoms exist. A photoemission study on the band structure of the sulfur overlayer [7] found that the lateral component of the sulfur 3p band has a large dispersion of 5 eV, from which there must be extremely strong, lateral bonds between the S atoms.

This, however, leads to a contradiction: The lattice constant of the overlayer of 3.5 Å is rather large, it is practically identical to the van der Waals diameter of sulfur [15] which should result in relatively weak interactions between the sulfur atoms. In order to account for this discrepancy the authors of the photoemission study suggested that the interaction may be enhanced by an unusual, substrate-mediated effect. On the other hand, it is not obvious why such an effect should be present here while it is absent in similar systems [16]. There was also a suggestion that a surface reconstruction may be involved where Al atoms occupy sites between the S atoms [17]. Using this model an electronic structure calculation reproduced the large dispersion of the $3p_{x/y}$ band seen in the experiment, however, the interstitial sites in the S layer appear too small for the Al atoms. The structure of the overlayer is therefore still an open question.

We have studied the sulfur/Al(111) system using scanning tunneling microscopy (STM). In the following we present data about the topography of the various phases which we found in addition to the one reported in the LEED study and about typical defects (Section 3.1). In Section 3.2 the nucleation and growth behavior of the S adlayer is investigated. Based on these observations we propose a novel structure model for the adlayer in Section 4. It is suggested that the S overlayer phases on Al(111) represent two-dimensional aluminum sulfides by which the incommensurability and presumably also the electronic structure can be rationalized.

2. Experimental

Experiments were performed in an ultra high vacuum (UHV) system, which contained the STM and was equipped with facilities for sample cleaning and with standard techniques for surface characterization. A clean and well ordered Al(111) sample was prepared by ion sputtering and annealing cycles, and the quality of the surface was controlled using Auger electron spectroscopy (AES) and LEED. For a complete and more detailed description of the sample preparation procedure and of the STM setup we refer to a previous publication [18]. The treatment of the sample prior to H_2S adsorption as well as the preparation of the tip was the same as in this former study.

The sulfur layers were prepared by reactive adsorption of H_2S following the procedure described by Jacobi et al. [7]. During deposition the sample was held at temperatures above room temperature, at 350 or at 570 K, in order to desorb the hydrogen from the dissociation of the H_2S molecules. Temperature-programmed desorption recorded after H_2S adsorption did not show additional hydrogen desorption, hence hydrogen desorbs fully during the reaction, at both temperatures. As seen with the STM there is also no qualitative difference in the types of structures formed at the two temperatures. In order to keep the background pressure low during the H_2S adsorption and to avoid contamination of the UHV system, the H_2S was introduced by a doser. It consisted of a stainless steel tubing at the opening of which the sample could be placed. The exposure for saturation of the Al(111) surface with sulfur was in

the 10^2 L range (1 langmuir = 1×10^{-6} mbar · s; exposures given in the figure captions are nominal numbers, corresponding to rises in background pressure and not to the actual pressure in front of the sample. In the former study no doser had been used, and saturation was reached after 10^4 L of H_2S [7].) S coverages were found to vary considerably across the sample surface, probably resulting from pressure inhomogeneities in front of the doser.

Auger electron spectra recorded as a function of H_2S exposure showed a continuous increase of the sulfur coverage until saturation. The Al LMM peak at 68 eV became asymmetric upon sulfur adsorption, and developed a shoulder at about 63 eV at higher coverages. A shift of the aluminum peak had been observed before and was interpreted as due to aluminum sulfide formation under the influence of the electron beam [7]. We could not find, however, any additional change of the low-energy shoulder after prolonged electron bombardement of the sulfur overlayers, only the S : Al peak height ratio was reduced. Hence, from our data the energy shift appears not to be caused by the AES electrons. The LEED pattern from the S-covered surface showed satellite spots around the substrate spots, identical to those observed by Jacobi et al. [7]. From our LEED data the lattice constant is 3.55 Å.

STM data are shown as gray-scale representations, with brightness according to height, or in pseudo three-dimensional views. Adsorption temperatures, nominal H_2S exposures and tunneling parameters are listed in the figure captions; the sign of the tunnel voltages corresponds to the potential of the sample with respect to the tip.

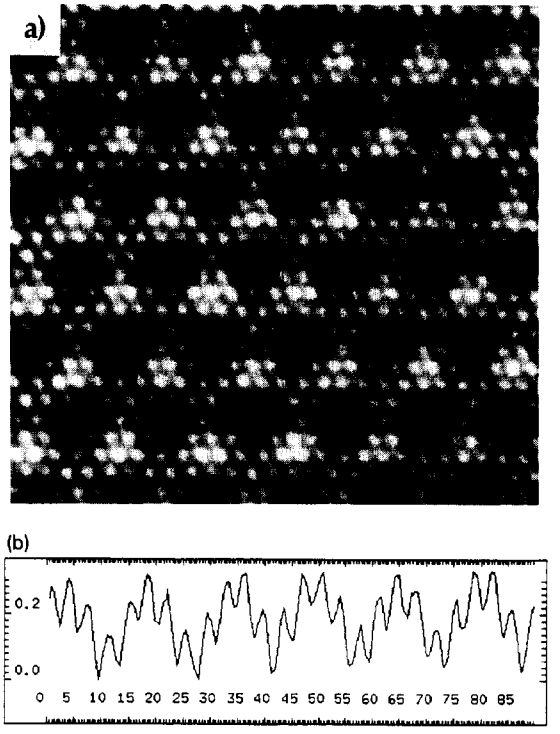

Fig. 1. (a) STM topograph of the non-rotated adlayer; (b) profile along a close-packed row. 92 Å × 87 Å, $I = 0.3$ nA, $V = -0.2$ V, $T_{ads} = 570$ K, 330 L H_2S.

3. Results

3.1. Moiré phases of sulfur on Al(111)

Fig. 1a shows an STM topograph of the Al(111) surface after exposure to H_2S at 570 K. It shows a hexagonal pattern which is superimposed by an additional structure with longer wavelength. From the lattice constant of about 3.5 Å of the hexagonal pattern this structure causes the hexagonal superlattice spots observed in LEED. The lattice parameters derived from the LEED pattern of 3.55 Å for the lattice constant and of 60° for the angles were therefore used for a precise calibration of the image axes. This yields 15.1 Å for the periodicity of the additional modulation. The corrugation amplitude of the atomic pattern is about 0.1 Å in Fig. 1a (see the line scan in Fig. 1b); this was found to considerably depend on tip conditions and on the tip-to-sample distance. The corrugation amplitude of the modulation structure is 0.2 Å in the topograph of Fig. 1. Values around 0.3 Å were found to be typical for the modulation amplitude and more or less the same for all of the ordered sulfur structures, and also largely independent of the sample bias voltage, indicating that it is not caused by electronic imaging effects. We ascribe the modulation structure to moiré fringes which result from the misfit between the larger hexagonal adsorbate layer and the smaller hexagonal substrate. The height modulation is then due to the various sites the adsorbate atoms occupy on the substrate, and the period of the moiré pattern corresponds to the distance between adsorbate atoms on

similar positions on the substrate. This interpretation is supported by the expected number for the wavelength of a moiré pattern formed by the superposition of two lattices, one with lattice constant 3.55 Å (d_S) and one with 2.86 Å (d_{Al}). Using $d_{moiré} = (d_S d_{Al})/(d_S - d_{Al})$ this yields 14.7 Å, in good agreement with the 15.1 Å derived from the STM images. The height modulation that is to be expected can be estimated from the positions that were calculated for S atoms on various sites on the Al(111) surface by Feibelman [14]. For on-top and hollow positions a difference of 0.45 Å (between the centers of the atomic cores) was found, somewhat more than the typical value derived from the STM images.

Fig. 1a contains two additional pieces of information: First, the moiré pattern is obviously parallel to the atomic rows of the overlayer. This means necessarily that the atomic rows of the overlayer must be parallel to the atomic rows of the substrate, too. With that we arrive at the same conclusion which had been drawn from the LEED observation that the overlayer and the substrate are aligned. Second, a careful inspection of the image shows that over the entire topograph the atomic arrangements in all maxima of the moiré pattern are different. That is, there are no two maxima (or minima) in the whole image which show exactly the same gray-level distribution over the atoms which form the maxima (or the minima), which can also be seen by the variation of the positions of the atomic maxima in the line scan of Fig. 1b. Hence, the moiré maxima cannot mark the unit cells of a periodic surface structure. As a consequence, the periodicity of the structure is either very large (larger than the area of the STM image which contains about 1000 substrate unit cells), or the overlayer is genuinely incommensurate. Since the overlayers are usually not perfect over distances much larger than the size of the topograph of Fig. 1, which is due to distortions, point defects, or steps (see below, Fig. 3), a discrimination between these two cases is meaningless. In the following we will use the term 'incommensurate', where we include the possibility of extremely large commensurate periodicities.

On other areas of the same surface it was found that the atomic pattern and the moiré fringes are rotated against each other. A typical case is shown in Fig. 2a. A rotated overlayer had not been detected in the former LEED/ARUPS study [7], and was also not observed with LEED in the present investigation. Note that the rotation of the moiré pattern, as seen in the image, is not identical to the rotation of the close-packed rows of the overlayer with respect to those of the substrate, as demonstrated in Fig. 2b. The line in the center of Fig. 2b runs along a close-packed direction of the substrate, the line below along a close-packed direction of the adlayer; the angle between is α. The upper line runs through atoms sitting about on on-top positions, corresponding to maxima of the moiré pattern; the angle with respect to the closed-packed direction of the overlayer is β, which is seen to be larger than α. β is the quantity that can be directly obtained from the STM images, α can be evaluated by using the expression derived in Fig. 2c. In Fig. 2a β is found to vary over the topograph, from 5° at the top to 2° at the bottom. With d_S taken to be 3.55 Å these values for β correspond to α values between 1° and 0.4°. These small values for α explain why a rotation had not been detected by LEED.

Our STM data show that on surfaces that are not fully covered by an S adlayer the rotational angles of the adlayer are limited to a range between 0° and 1°. Atomic steps often represent boundaries between domains of different orientation, but the rotation was found to change also in a continuous way on the terraces as can be seen in Fig. 2a. In such continuous transitions defects in the adlayer play an important role. This is illustrated by Fig. 3 showing a section with an edge dislocation. The additional row of atoms runs from the lower left corner to some point in the middle of the image (additional row marked by an arrow) where it ends close to one of the point defects. The edge dislocation in the atomic lattice is at the same time an edge dislocation also for the moiré fringes: An additional row of moiré maxima emerges from the point defect, in the direction opposite to the row inserted into the atomic pattern. Closer inspection of Fig. 3 reveals that the adlayer reacts to the edge dislocation by changing the rotational angle: From 0° at the area at and closely above the additional row to 1° above the end point and to −1° below it. (The changes in the directions between the atomic rows and the moiré pattern can best be seen by viewing the image at a flat angle.) The transitions between the orientations are not sudden

but extend over several periods of the moiré phase. It appears that, for angles between 0° and 1°, it costs relatively little energy to rotate the adlayer against the substrate. Besides the incommensurability itself this is further evidence for the flatness of the adlayer–substrate potential.

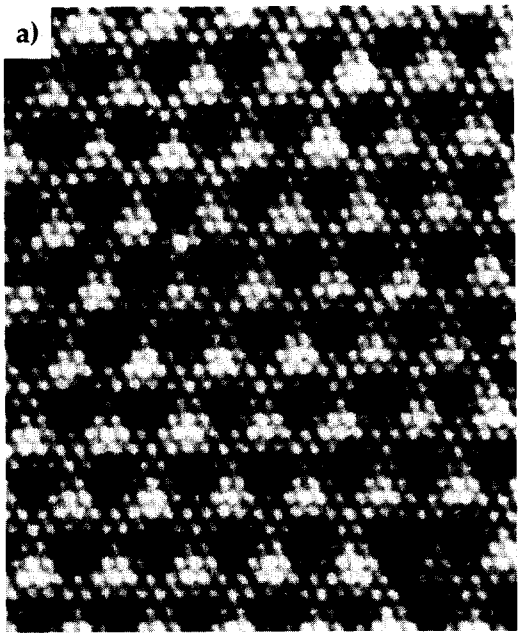

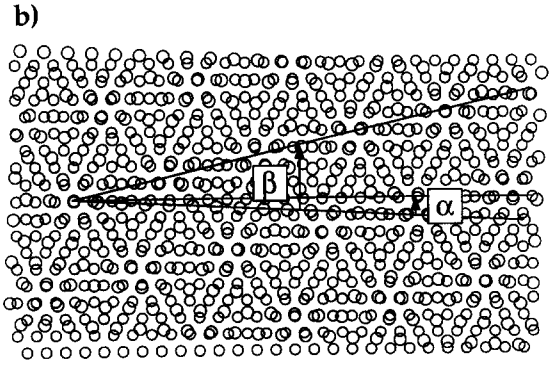

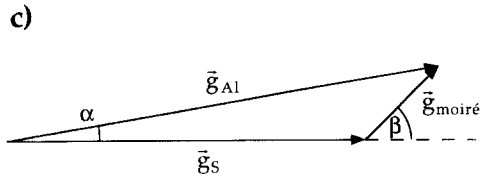

Fig. 2. (a) STM topograph of the slightly rotated adlayer. 102 Å×125 Å, $I = 0.3$ nA, $V = -0.2$ V, $T_{ads} = 570$ K, 330 L H_2S. (b) Superposition of two hexagonal lattices with different lattice constants and slight rotation; larger circles indicate the top, smaller circles the bottom layer; β is the angle of the moiré pattern against the close-packed direction of the top layer, α is the angle of the close-packed direction of the top layer against the close-packed direction of the bottom layer. (c) Construction of α from β (equivalently to the treatment by Ostyn and Carter [40]): The reciprocal lattice vector of the moiré pattern ($g_{moiré}$) is the difference between the reciprocal lattice vectors of the aluminum substrate (g_{Al}) and the overlayer (g_S). This yields $\tan\beta = (-|g_{Al}|\sin\alpha)/(|g_S| - |g_{Al}|\cos\alpha) = [\sin\alpha]/[\cos\alpha - (d_{Al}/d_S)]$ from which α can be evaluated using $d_{Al} = 2.86$ Å, and d_S and β from LEED and STM. For small angles the expression simplifies to $\alpha = [(d_S - d_{Al})/d_S]\beta$.

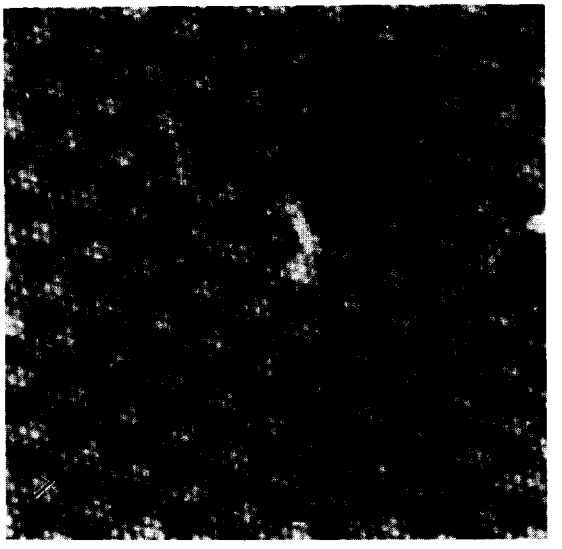

Fig. 3. STM image of a section containing an edge dislocation in the adlayer; the arrow marks the inserted row; 150 Å×144 Å. $I = 0.3$ nA, $V = -0.2$ V, $T_{ads} = 570$ K, 330 L H_2S.

At coverages in the saturation regime of the sulfur AES intensity we observed much larger rotational angles of the moiré pattern, clearly outside the range of angles between 0° and 1°. An example is shown in Fig. 4. The lower half of the image shows the slightly rotated structure known from the smaller coverages, whereas the upper half represents a new structure. Its lattice parameters were evaluated based on the calibration of the image using the slightly rotated phase in the lower half. This gives 3.47 Å for the atomic lattice and 12.4 Å for the periodicity of

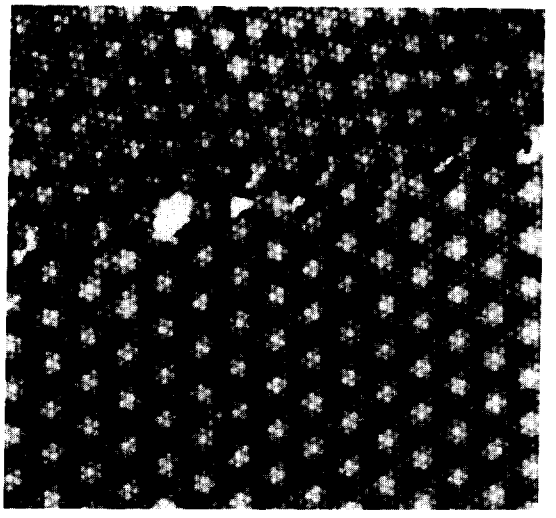

Fig. 4. STM topograph showing a compressed, more strongly rotated phase at the top and a slightly rotated phase at the bottom. 183 Å×178 Å, $I = 0.01$ nA, $V = -0.9$ V, $T_{ads} = 570$ K, 450 L H_2S. For the rotational angle the exact expression from Fig. 2c has to be used. Furthermore, in order to apply the construction from Fig. 2c, the angle between the moiré and the atomic lattice of the compressed phase has to be measured in such a way that a substrate vector is between them, as shown in Fig. 2b. (The direction of the substrate is roughly known from the lower half of the image.)

the moiré pattern. For the rotational angle β numbers between 37° and 47° are found which, using Fig. 2c, corresponds to about 8° for the angle α between the lattices. This compressed structure is also (virtually) incommensurate with the substrate. Such structures, which represent higher coverage phases, were detected only after prolonged exposure of the Al(111) sample to H_2S, where areas of free aluminum do no longer coexist with the S-covered areas. Also in the higher coverage regime two further structures were observed (not shown here). Since these were obtained only as relatively small patches their structure parameters could not be determined with the same precision as for the other phases. We find 2.5° and 5° for the rotational angle α and about 3.5 and 15 Å for the atomic lattice constants and the moiré periodicity, respectively. Neither these phases nor the compressed structure described above were seen in the LEED pattern. This is probably due to the fact that for the H_2S exposures applied in this study and also in the former investigation [7], these phases remained minority species with coverages too low to be detected by LEED. Table 1 lists the structure parameters of the various phases which could be identified in the STM images.

Table 1
Lattice parameters of sulfur phases on Al(111)

Overlayer lattice spacing (Å)	Moiré lattice spacing (Å)	Rotational angle (α) (deg)
3.55	15.1	0–1
3.5	15	2.5
3.5	15	5
3.47	12.4	8

Fig. 5 shows two point defects which are typical for the adlayer, some of which could also be seen in Fig. 3. They have a characteristic shape consisting of a bright point surrounded by a dark ring. In Fig. 5 it is seen that the bright point corresponds to an atom of the adlayer which is imaged with a greater height (the bright spot is exactly in phase with the atomic lattice), and the dark ring to the six atoms around this feature, which are imaged lower. This might be due to a variation in actual height of the atoms, or to a variation in state density at the defect. All of these defects have a distinct phase relation with the moiré pattern, they are always located in the minima. These observations would be hard to rationalize if the adlayer were in fact a simple layer of S atoms. Intrinsic point defects of a simple sulfur layer are

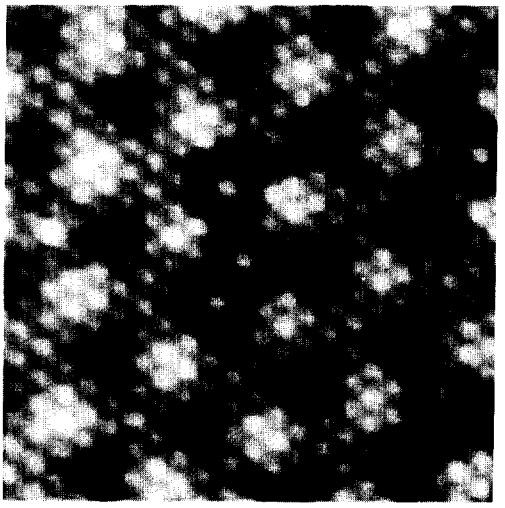

Fig. 5. Image showing two point defects in the adlayer. 66 Å×56 Å, $I = 0.1$ nA, $V = -0.9$ V, $T_{ads} = 570$ K, 450 L H_2S.

either S interstitials or S vacancies. In the case of interstitials the defects should be located between the atoms of the overlayer, S vacancies should be imaged dark because the adlayer appears higher in the topographs than the bare metal surface (see below, Fig. 7); both is in contrast to observation. Alternatively, the defects could be due to contaminant atoms underneath the adlayer, e.g., C atoms which always exist in small quantities on the aluminum surface [18]. However, this contradicts the positions of the defects in the moiré minima, since the C atoms are randomly distributed on the clean surface and strongly bound to their sites and should, therefore, show no correlation with certain positions of the overlayer. Furthermore, the defects show clustering on a larger scale (see below, Fig. 10), also contrasting the random distribution of typical foreign atoms [18]. This rules out also foreign atoms in the adlayer itself, originating, e.g., from a small contamination of the H_2S gas, which should again show a random distribution. In Section 4 it will be proposed that the characteristics of the defects can be rationalized quite naturally if the adlayer consists of several layers.

3.2. Nucleation and growth of the sulfur adlayer

In this section we present data about the formation mechanism of the sulfur adlayer. Since H_2S was introduced into the system via a doser directed at the sample manipulator from which the sample had to be transferred to the STM after the dosing all data are ex situ results obtained after adsorption. Fig. 6 shows an STM topograph which was recorded after a very small amount of H_2S had been adsorbed. Sulfur could, however, already be detected by AES. The surface is still mostly bare aluminum, the two monoatomic steps in the image have the same irregular shape which is typical also for the clean Al surface. Moiré phases have not yet developed so that sulfur must be represented by the small, bright features. Since these show a distribution of sizes and shapes, and many of them also a fine structure, they cannot represent individual S atoms which should all appear equal and without an internal structure. From their typical diameters of a few Å we interpret them as clusters consisting of few sulfur atoms. Only the smallest ones can possibly be individual atoms.

Fig. 6 shows that most of these clusters are

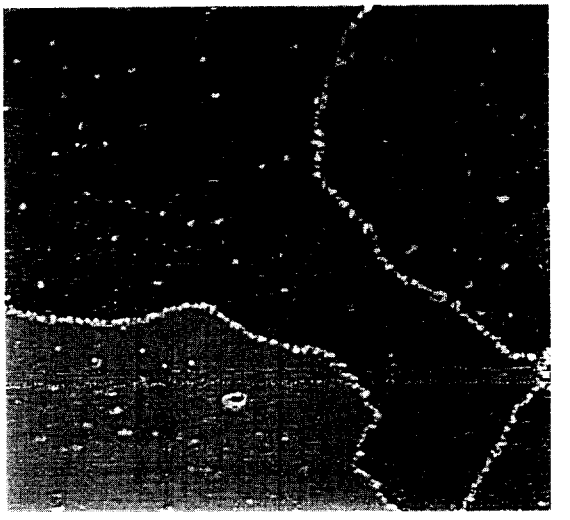

Fig. 6. Image of the Al(111) surface after deposition of a small amount of H_2S. Bright features at the step and on the terraces are due to S clusters. 700 Å × 640 Å, $I = 1$ nA, $V = -1.5$ V, $T_{ads} = 570$ K, 12 L H_2S.

localized at the upper edges of the steps (steps are descending from left to right), while their concentration on the terraces is considerably lower. In principle, this could result from a higher dissociation probability of H_2S molecules or from a greater thermodynamic stability of the clusters at these sites. The latter explanation is supported by the observation that the same distribution of clusters was observed when bulk sulfur was segregated to the surface by prolonged annealing of the crystal. The complete decoration of step sites by small amounts of sulfur is of importance for the well known fact that sulfur is an efficient poison for many catalytic reactions on metal surfaces [19,20]. Some of these reactions, e.g., the dissociation of hydrocarbons [21], are known to proceed preferentially at low-coordinated sites such as at steps and kinks. Fig. 6 demonstrates that exactly these most reactive sites are first blocked by the sulfur. In such a case the effect of a sulfur contamination is much larger than expected if only its mean coverage is considered.

Fig. 7 shows an STM topograph of a surface which, according to AES, has a somewhat higher sulfur coverage than that in Fig. 6. The STM topograph shows, in addition to the clusters seen already in Fig. 7, a small, triangular island of the moiré structure which has apparently grown at the defect

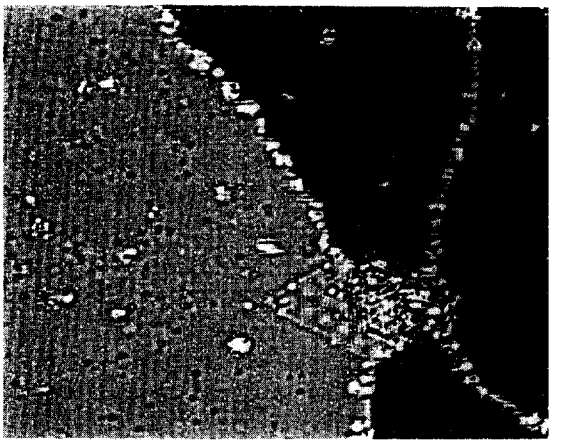

Fig. 7. Small island of the incommensurate adlayer and clusters of S atoms. 336 Å×266 Å, $I = 0.1$ nA, $V = -1.4$ V, $T_{ads} = 570$ K, 60 L H_2S.

Fig. 8. Adlayer islands growing at steps of the aluminum surface. 470 Å×370 Å, $I = 1$ nA, $V = -1.5$ V, $T_{ads} = 350$ K, 6 L H_2S.

between the two steps. (The faint, dark features on the terraces are due to single atoms of a small amount of contamination on the Al(111) surface [18].) Nucleation of moiré islands was generally observed when all step sites were fully covered by the clusters. The most important result from Fig. 7 is that the brightness, i.e., the apparent heights of the clusters and of the moiré island with respect to the metal layer are different: The clusters are imaged about 2 Å higher than the metal surface, which was found to be a typical value for various tunneling conditions and to be largely independent of the polarity of the tunneling voltage. The average height of the moiré island in Fig. 7 is only 0.1 Å, but a more typical value is about 0.5 Å. This difference in height between the clusters and the moiré islands is significant and was found under all conditions. It means that either the geometric positions of the atoms in the clusters and in the moiré phases with respect to the substrate atoms are different, or that the two features have different state densities and hence electronic structures. In any case sulfur adopts two clearly different states. When the initially formed clusters represent small groups of adsorbed sulfur atoms it is clear that the moiré phases must be something else.

With increasing coverage the moiré islands continue to grow, mostly along the steps. This is demonstrated in Fig. 8. The adsorption of H_2S was performed at 350 K in order to identify possible activated processes in this stage of the reaction more clearly. This explains the poorer order of the adlayer compared to that at 570 K. The smaller features on the bare parts are the clusters typical for the low

Fig. 9. Atomically resolved image of the border between the adlayer and the clean aluminum surface. 198 Å × 82 Å, $I = 0.3$ nA, $V = -1.5$ V, $T_{ads} = 350$ K, 6 L H_2S.

coverages. Fig. 8 shows that the steps are now completely decorated with moiré islands; the clusters which must have existed at these areas apparently became incorporated into the moiré adlayer. From this image it is obvious that the steps play an important role in the formation mechanism of the moiré structures.

Figs. 7 and 8 show that the moiré phases form islands. Hence, there must be attractive interactions between the atoms inside the sulfur adlayer. Fig. 9 allows, in addition, to draw certain conclusions about the characteristics of these interactions. The topograph was recorded on a two terrace area of the surface, the horizontal black-and-white stripe represents the step. Most of the area is covered by the moiré adlayer, however, there is a stripe of bare aluminum in the center of the image. First, it is seen that the boundary between the sulfur adlayer and the bare aluminum is stable. This is indeed different from many other systems which show a 'frizzyness' of the edges of islands or steps [22]. Such an effect is seen in Fig. 9 only at very few positions, and it affects only individual atoms, e.g. at the tip of the small, triangular island in the right half of the image. 'Frizzles' in STM images are mostly a dynamic effect and indicate diffusion of the atoms on a time scale shorter than the time between two successive scan lines. The fact that the 'frizzles' are almost absent here evidences that the atoms at the edges of the islands feel strong bonds which keeps them on their sites and, therefore, have to sit in deep potential minima. The energy can be estimated from the number of hopping events in the STM image and the mean observation time for the edge atoms. With a preexponential factor of 10^{13} s^{-1} we estimate about 0.7 eV. If there were only van der Waals bonds the boundaries of the islands would fluctuate heavily on the time scale of the STM experiment.

Furthermore, Figs. 7, 8, and 9 display a strong tendency of the islands to adopt a triangular shape. This corresponds to a symmetry reduction from the six-fold rotational symmetry of a free standing hexagonal layer to a three-fold one. This is caused by the fact that the (111) surface of an fcc solid has only a three-fold symmetry by which island edges along the closed-packed directions $[1\bar{1}0]$ and $[\bar{1}01]$ are inequivalent, and therefore have different stabilities.

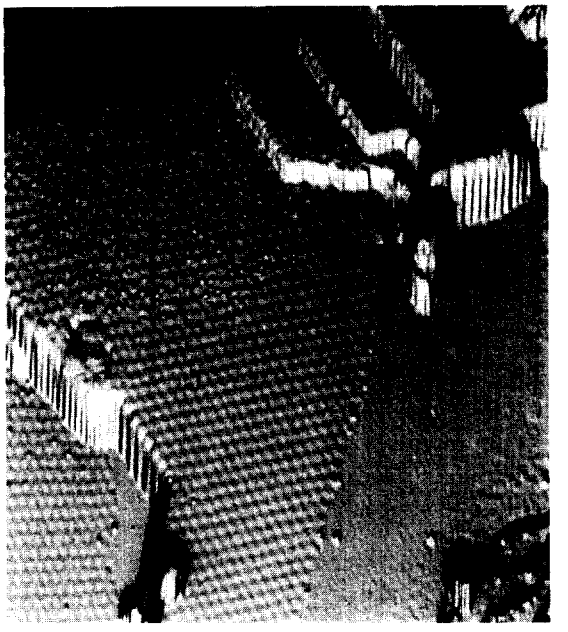

Fig. 10. Large-scale STM image of the partially S-covered surface; the area in the center is the defect-free moiré structure, top: moiré structure with many point defects, area to the right: clean aluminum. All steps are multisteps. 560 Å × 580 Å, $I = 0.3$ nA, $V = -2.1$ V, $T_{ads} = 570$ K, 24 L H_2S.

Finally, Fig. 10 shows a topograph recorded after adsorption at 570 K. The areas in the image center and at the lower left corner are covered with an almost perfect moiré layer, whereas the moiré structure at the upper half has a large number of the defects which were described above (Fig. 5). The area to the right is clean aluminum. As expected for the higher temperature, the order of the surface is generally better than after adsorption at 350 K. Furthermore, all of the steps seen in Fig. 10 are multilayer steps – the three smaller ones in the upper half are bilayer steps, the two larger ones are six layers high, and the steps are straight and run mostly parallel to the moiré pattern. Multilayer steps and the alignment of steps were found to be typical for higher coverages of sulfur and for the higher temperature. On the other hand, on the clean Al(111) surface almost exclusively monolayer steps are found, with very irregular directions. Therefore the overall topography of the surface changes upon adsorption of sulfur. There are two possible explanations for this finding: In a thermodynamic picture certain facets become energetically stabilized. This can be under-

stood when particularly stable sulfur structures form at step edges, which would then grow to larger microfacets, or when larger (111) terraces become stabilized relative to small ones by the moiré adlayer, by which the system would try to reduce the step density. Alternatively, the facetting can be connected with the formation mechanism of the moiré adlayer. This is to be expected when the adlayer involves a reconstruction where the density of metal atoms in the surface layer is different from that in a substrate layer. In such a case the surface topography has to change during the formation of the moiré structure because of transport processes of substrate material. If these processes are partially suppressed at areas where moiré islands have already formed this would also lead to a facetting.

4. Discussion

The STM data show that sulfur forms adlayers on Al(111) which have no common periodicity with the substrate lattice across areas of at least 1000 substrate unit cells. The adlayer is therefore incommensurate, from which it has to be concluded that the adlayer–substrate potential must be relatively flat, i.e., the corrugation amplitude of the potential and therefore the forces by which the substrate atoms act on the adlayer atoms are small compared to the forces between the adlayer atoms.

An incommensurate structure of S adsorbed on Al(111) had been concluded before from LEED and ARUPS observations [7]. This former study found, however, only one phase, with the crystallographic axes parallel to those of the substrate. The STM results demonstrate that the adlayer may adopt also other orientations with respect to the substrate. From our data small rotations, between 0° and 1°, are caused by defects such as edge dislocations, whereas larger rotations are connected with an increasing sulfur coverage. A relationship between the orientation and the coverage of an adlayer, the so-called 'rotational epitaxy', has been studied for the better known incommensurate systems of adsorbed noble gases [8–11] and alkali metals [12,23]. It is found that, for given coverages and therefore for given lattice constants, these systems exhibit defined rotational orientations of the adsorbate layer with respect to the substrate. Various theoretical concepts have been developed to find relationships between the lattice constants and the angles: Fuselier et al. [24] and Doering et al. [23,25] treated systems which are in fact commensurate but have very large unit vectors. The rotation arises from a locking-in of the overlayer into positions where some adsorbate atoms sit on high symmetry sites. The rotation is therefore a discontinuous function of the coverage, i.e. of the lattice constant. Ideal incommensurate systems, with no common periodicities, were treated by Novaco and McTague [26,27]. Also in this case non-zero angles occur, but the rotational angle is a continuous function of the lattice constant.

Experimentally we find four different phases which are listed in Table 1. The data suggest that the rotational angle increases with decreasing lattice constant, although more data are needed to identify a clear trend. The fact that no continuous rotation is observed seems to contradict the predictions by Novaco/McTague and to support a locking-in of the adlayer for certain angles. However, under the conditions where the adlayer grows, the system is certainly not fully in thermodynamic equilibrium as assumed by the theories. Since the internal bonds in the adlayer must be strong, the activation energy to press further atoms into the layer must be large, which is expected to lead to oversaturation effects and to an island growth mechanism. That this is actually the case follows from the observation that always several phases coexist (see Fig. 4), indicating that the denser phases grow in islands surrounded by less dense areas. On the other hand, systems such as physisorbed noble gases [8,10,12,23] and adsorbed alkali metals [9,11] appear to be less subject to such kinetic effects. The difference is apparently due to the chemical nature of the adlayer atoms which in the case of Al(111)/S cause very strong internal bonds. Nevertheless, our data suggest that sulfur adsorbed on Al(111) in fact shows rotational epitaxy, which is a typical property of incommensurate systems.

A structure model for Al(111)/S must therefore explain a small corrugation of the adlayer–aluminum potential in comparison to the strength of the internal interactions within the adlayer. A number of structure models is shown in Figs. 11 and 12. The structure in Fig. 11a is a simple adlayer of S atoms

(large open circles) on the aluminum substrate (smaller gray circles). In the model shown in Fig. 11b the adlayer consists of one layer of S atoms and one layer of Al atoms (darker shading) laterally expanded from the lattice constant of the substrate of 2.86 Å to that of the adlayer of about 3.5 Å. This is the type of structure for which an electronic structure calculation had been performed by Bullett [17]. In this study, in addition, the distance between the S and the Al layer was varied. Another structure not shown in Fig. 11, with the expanded Al layer on top of the S layers, has also to be considered. The model shown in Fig. 12 is a sandwich structure of two S layers (large open circles) with an aluminum layer (smaller dark circles) in between. Fig. 12a is a top-view (topmost layers successively cut away), Fig. 12b a side view (brighter gray circles represent the substrate atoms). In all multilayer models each layer has to be hexagonal and must have the same lattice constant of about 3.5 Å of the complete adlayer. Otherwise additional periodicities would be superimposed which were absent in the STM images.

As we have already pointed out in the introduction, a simple layer of S atoms leads to contradictions between the incommensurability of the adlayer and its electronic structure on the one hand and the

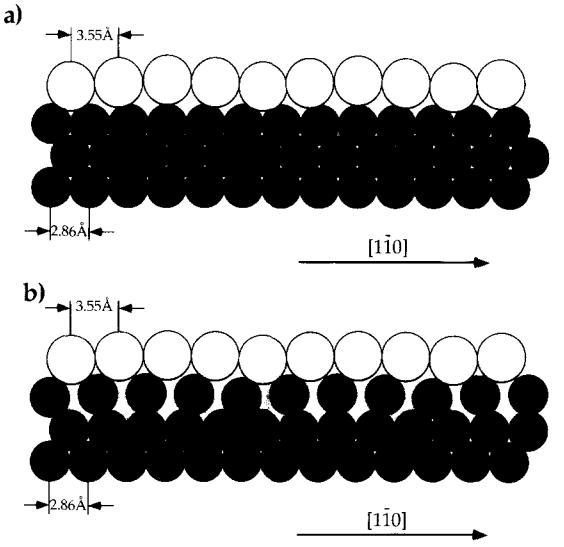

Fig. 11. Structure models: (a) Simple adlayer of S adatoms (large white circles) on the Al substrate (smaller gray circles). (b) Bilayer consisting of S atoms and an expanded layer of Al atoms (dark gray circles).

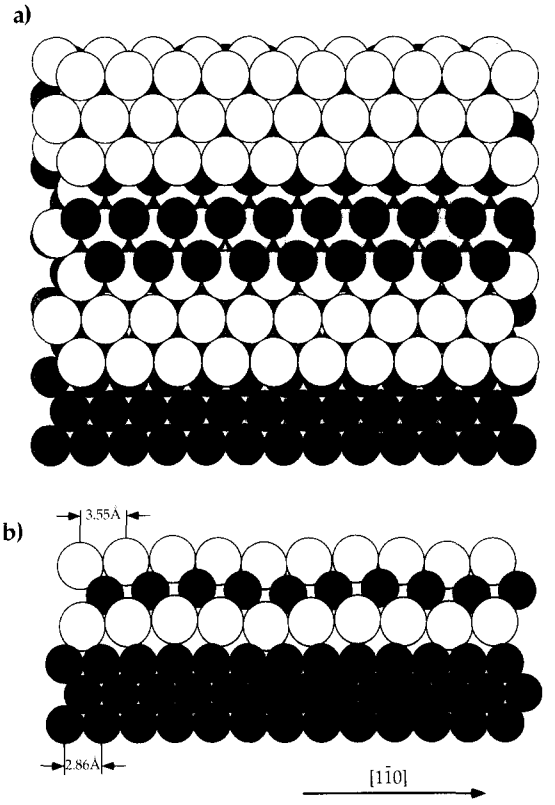

Fig. 12. Sandwich structure from two sulfur layers and one Al layer; large white circles are S atoms, dark gray circles adlayer Al atoms, lighter gray circles Al substrate atoms. (a) Top view: the topmost layers are partially cut away, (b) side view.

character of the sulfur–metal bond and the large lattice constant of the adlayer on the other hand. Since the absolute imaging height of adsorbates in STM does not provide any direct structure information we can, of course, not discriminate between the various structure models simply by the images of the adlayer. However, our data do provide evidence against a simple layer of S atoms and for a multilayer structure that comprises at least one S and one Al layer, such as those shown in Figs. 11b and 12: A multilayer structure is supported by the fact that the typical point defects are directly at the positions of the surface atoms. The defects could, e.g., be due to interstitial atoms directly underneath the surface atoms, or, in the model of Fig. 12, to S atoms in the second layer which are replaced by Al atoms. On the other hand, it is difficult to reconcile the positions of the defects with a one-layer structure as was shown

in Section 3.1. Furthermore, the imaging height of the adlayer with respect to the bare metal surface is significantly different from the height of the clusters observed in the beginning of the adsorption. If the clusters represent groups of adsorbed surface S atoms, the moiré phases must be structurally or chemically different. This supports a multilayer structure where Al atoms in the adlayer affect the chemical state of the S atoms. The small apparent height of the moiré islands with respect to the bare aluminum of typically 0.5 Å can be explained by a lower density of states at E_F compared to the uncovered metal. It is also possible that the bare metal around the moiré islands is one aluminum layer higher than the substrate underneath the island, i.e., the island borders are substrate steps at the same time. Another argument is the activation energy that is connected with the formation of the adlayer, the presence of which was concluded above from the nucleation of the moiré islands at the steps. For a multilayer structure site exchange reactions between S and Al atoms must take place which are faster at steps because of the lower coordination number of step atoms. It is clear that such an effect is absent for a simple S adlayer. Another possibility for an activated step is the dissociation of the H_2S molecules. However, we have shown above that the decoration of steps by the initially formed clusters is probably not caused by a preferred dissociation of molecules at steps, but by a greater stability of these features at step sites. We conclude that a possible site selectivity of the dissociation of the molecules is probably not important for the distribution of any sulfur features on Al(111) under the present reaction conditions. In addition, as a consequence of the smaller number of Al atoms per unit area in the adlayer compared to a layer in the substrate (see the models in Figs. 11b and 12) transport processes of aluminum atoms have to occur. These reactions are expected to involve at first the metal atoms at the steps, which has been shown for adsorbate induced reconstructions on other surfaces [28]. These sites are, however, quickly used up because of the nucleation of moiré islands at the steps. If we assume that the moiré islands in part stabilize the surface against removal of aluminum atoms further Al atoms have to come from clean terraces, where also several layers may be removed. This provides an explanation for the formation of multilayer steps without the need to assume a stabilization effect of sulfur on certain facets.

Our data therefore point to an adlayer structure for the moiré phases on Al(111) which is composed of S and Al layers. Since the STM does not allow for a chemical identification of the atoms, we are, however, not able to discriminate directly between several possible multilayer models. We favor, however, a model of the type of Fig. 12. In such a sandwich structure Al atoms are completely surrounded by sulfur atoms so that, because of the electronegativity of sulfur, the bonding should be partially ionic. Such an adlayer is more properly termed a surface sulfide. This would explain the chemical shift of the Al LMM peak which was observed in the AES. The direction of the shift is the same as for aluminum oxide [18]. Its magnitude is smaller, however, as is expected because of the smaller electronegativity difference between Al and S. The structure of the surface sulfide suggested here can be derived from bulk aluminum sulfides, Al_2S_3. Three ambient pressure modifications have been described [29,30] of which α- and β-Al_2S_3 have defect wurtzit structures (the α-form has an ordered occupation of cation sites, the β-form a statistical occupation), and γ-Al_2S_3 which has a corundum structure. Common to all three modifications is that they contain hexagonal S layers with the Al atoms on different sites between them; S–S distances are 3.71, 3.60, and 3.74 Å, i.e., they are somewhat larger than the lattice constants of the overlayers between 3.55 and 3.47 Å. The cations in Al_2S_3 occupy tetraheder (for α and β) or octahedron sites (for γ) between the S layers; the coordination of Al in the surface sulfide is unknown so far. For stoichiometry reasons the cations in the bulk sulfides form only incomplete hexagonal layers, which might account for the somewhat larger S–S distances. In spite of the similarities the adlayer sulfide proposed here is therefore a distinctly different phase which is restricted to the two-dimensional case.

A sulfide-like adlayer can also explain findings about the elastic properties of the adlayer: The fact that the point defects show clustering is explained by strain effects caused by other surface defects such as steps, if, e.g., these have some unfavorable direction. The distribution of these defects (Fig. 10) indicates that these effects may be quite far-reaching. A lower

limit for the range of strain caused by point defects can be derived from the observation that the defects are always located in the minima of the moiré structure, from which the range must be in the order of a period of the moiré structure of about 15 Å. This lower limit is compatible with the behavior of the adlayer at edge dislocations (Fig. 3) where the transition lengths between areas of different rotational angles extend over several moiré periods. Hence, defects cause far-reaching distortions from which we conclude that the modulus of elasticity of the adlayer must be quite large. It is clear that in a sulfide-like adlayer the stiffness should be larger than when only van der Waals bonds act between the particles.

In a sulfide-like adlayer strong chemical bonds should exist between the layers of S and Al atoms. This is directly reflected by the stability of the adlayer island edges indicating that the S atoms are immobile and in deep energy minima, of the order of 0.7 eV, as was estimated above from the fluctuation rate. Because of the flat adsorbate–substrate potential it is not possible that these minima are provided by the substrate. Hence the adlayer atoms must be hold on their sites by strong lateral bonds, between the atoms in the islands. The magnitude of these interactions exceeds by far van der Waals energies of a few 10 meV that have to be expected for direct interactions between S atoms about 3.5 Å apart [15]. It also exceeds energies found for substrate-mediated adsorbate–adsorbate interactions. For example, for oxygen/Ni(100) attractive or repulsive interactions in the order of k_BT have been estimated for O atoms on (2×2) or $c(2 \times 2)$ sites, respectively [31]. The immobility of the oxygen atoms in this case is a result of the corrugation of the substrate potential. For the sulfur moiré phases on Al(111) we explain the magnitude of the interactions between the adlayer particles by the chemical bonds between the sulfur and the aluminum atoms in the adlayer. Consequently, a considerable part of the adsorption energy of the sulfur is localized in internal bonds, within the adlayer, while the bonding of the adlayer as a whole to the substrate is weaker. In the extreme, for a complete internal saturation of bonds only van der Waals interactions remain for the bonding of the adlayer to the substrate. It is clear that in such a case the lattice parameters of the adlayer will be largely determined by the coordination and bond lengths characteristic for the internal chemical bonds in the adlayer, and not by the adsorbate–substrate potential. This is exactly the prerequisite that an incommensurate overlayer can be formed. It is clear, however, that studies using other methods are necessary to confirm such a model.

A sandwich structure resembles to some extent that of layered disulfides of group IV, V, and VI transition metals, such as MoS_2: These consist of hexagonal layers of sulfur where every two layers have a layer of metal atoms between them. The bonding of the metal atoms to the chalcogen atoms is covalent but has ionic contributions, the bonding between the sandwich layers is of the van der Waals type. S–S distances are between 3.15 and 3.66 Å [32], i.e., the lattice constants of the S phases on Al(111) are in the same range.

Finally, any structure model has to explain the unique electronic structure which has been found for the sulfur adlayer. In the ARUPS investigation by Jacobi, Muschwitz, and Kambe [7] a dispersion of the sulfur 3p band, of about 5 eV, has been reported, in clear contrast to expectation for an adlayer of S atoms which are 3.5 Å apart. A tight-binding calculation performed by the same authors showed that, in order to reveal the experimental magnitude of the dispersion, the overlap integral between the S atoms would have to be twice as large as that between the Se atoms in the $c(2 \times 2)$/Se structure on Ni(100). This structure has almost the same lattice constant (3.52 Å), however, the dispersion is only 1.6 eV [16]. It was suggested that anomalous substrate-mediated interactions in the case of the Al(111) surface may be responsible, however, only a simple S layer was considered. A different idea was put forward by Bullett [17], which was based on a bilayer model for the adlayer, similar to that shown in Fig. 11b. The author studied the effect on the electronic structure upon varying the distance between the two layers. It turned out that the experimental dispersion of the $3p_{x/y}$ band could only be obtained, when the two layers are almost coplanar, i.e., when the Al atoms are located almost exactly between three S atoms. The problem with that model is that for such a geometry the S–Al distance can be only 2.05 Å, whereas the sum of the radii of S and Al atoms is significantly larger; for covalent bonds it should be 2.30 Å, for ionic bonds 2.34 Å [15]. It is

hard to predict whether the introduction of a second layer of S atoms (Fig. 12) is sufficient to increase the lateral interactions between the S atoms by the amount required to explain the band width, without the need of assuming unrealistically small distances between the Al and S atoms. The presence of two sulfur layers certainly increases the ionicity of the bonding within the adlayer and possibly also the interactions between the S and the Al atoms and by this also between the S atoms. Interestingly, large widths of the S 3p band have been found in calculations for the group IV, V, and VI layered disulfides: e.g. for MoS_2 values between 5 and 7 eV were reported although the metal–S distances are not small [33]. In fact, the situation in these compounds is more complex, because the metal d-states mix with the sulfur p-states in this band. The analogy to these layered bulk sulfides should therefore not be stretched to far.

An incommensurate sulfide adlayer is quite unique; the formation of sulfides instead of chemisorbed S layers is known from other surfaces, however, also in these cases the surface structures have relatively small unit cells. Examples are the $(\sqrt{7} \times \sqrt{7})R19°$ structures on Pd(111) [34,35] and on Cu(111) [36,37]. On the other hand, (virtually) incommensurate structures occur not only for physisorbed noble gases, adsorbed alkali metals or certain metal-on-metal systems, where the bonds to the surface are either very weak (for the noble gases) or not very directional (for the alkali metals and the metallic systems). Non-coincidence overlayers have been observed, e.g., for films of FeO on a Pt(111) surface [38] and for graphite on Pt(111) [39]. Both are systems where the bonds of individual atoms (oxygen or carbon) to the substrate are strong and directional. However, internal bonds are even stronger in these cases, by which the adlayers can gain more by optimizing their lattice constants than by trying to adapt to the substrates. A further aspect for the difference between S/Al(111) and the quoted examples of sulfide layers is the presence of d-states in the metals. These lead to more directional bonds between the adlayer and the substrate and therefore favor locking-in of the overlayer. Because of the near free-electron character of aluminum the interaction potential with an adsorbate layer is expected to be less corrugated.

5. Summary

We have shown that overlayers formed by reactive adsorption of H_2S on an Al(111) surface are incommensurate, confirming former observations by LEED and ARUPS [7]. However, not only a structure with crystallographic axes parallel to the substrate directions was observed, but additional, rotated phases. For small angles between the axes, between 0° and 1°, continuous rotations were found, which are caused by defects such as edge dislocations in the adlayer. Larger rotational angles were found with increasing S coverages, the angle increases from between 0° and 1° for the initially formed phases (lattice constant 3.55 Å) to 8° after prolonged exposure to H_2S (lattice constant 3.47 Å). This is explained by rotational epitaxy known from other incommensurate systems; the fact that no continuous rotation was observed for these larger angles is most likely caused by kinetic effects. The observations indicate a flat adsorbate–substrate potential, quite unexpectedly for the bonding of sulfur to a metal surface.

The STM data reveal evidence that the adlayer is not a simple layer of S atoms, but is composed of several hexagonal sulfur and aluminum layers: The shape of characteristic point defects and their locations at the atomic positions of the adlayer cannot be explained by intrinsic defects of a simple S layer. Furthermore, the adlayer is imaged differently from the clusters of S atoms formed in the beginning of the reaction. The fact that the adlayer nucleates at step edges indicates that activated processes play a role. These are probably not caused by the dissociation of the H_2S molecules, but by exchange reactions between S and Al atoms which have to occur for a multilayer structure involving aluminum atoms. In addition, because the density of Al atoms in the adlayer is different from that in the substrate, transport processes are necessary which explain the partial facetting of the surface observed after reaction with H_2S.

While from the STM topographs alone several multilayer models are possible we suggest a sandwich structure of two S layers with an Al layer in between. By this we are able to explain a number of further findings: The shift of the AES Al LMM peak points to ionic contributions to the chemical bonding

in the adlayer, and the distance between neighboring S atoms is similar to that of various bulk Al_2S_3 modifications. From the response of the adlayer to lateral strain a considerable stiffness of the adlayer is derived. The formation of adlayer islands and the stability of the island edges evidence attractive interactions between the atoms in the adlayer which are much larger than expected if only direct or substrate-mediated interactions act between neighboring S atoms. All these observations are compatible with the picture that the adlayer represents a two-dimensional sulfide, with strong internal bonds between the S and Al atoms. We suggest that the structure is similar to that of layered transition metal disulfides such as MoS_2. This may presumably also account for the unique electronic structure which had been reported for the S/Al(111) system [7].

References

[1] J.E. Demuth, D.W. Jepsen and P.M. Marcus, Phys. Rev. Lett. 32 (1974) 1182.
[2] W. Heegemann, K.H. Meister, E. Bechtold and K. Hayek, Surf. Sci. 49 (1975) 161.
[3] P.C. Wong, M.Y. Zhou, K.C. Hui and K.A.R. Mitchell, Surf. Sci. 163 (1985) 172.
[4] C.M. Chan and W.H. Weinberg, J. Chem. Phys. 71 (1979) 3988.
[5] F. Macá, M. Scheffler and W. Berndt, Surf. Sci. 160 (1985) 467.
[6] L. Ruan, I. Steensgaard, F. Besenbacher and E. Lægsgaard, Phys. Rev. Lett. 71 (1993) 2963.
[7] K. Jacobi, C.v. Muschwitz and K. Kambe, Surf. Sci. 93 (1980) 310.
[8] C.G. Shaw, J.S.C. Fain and M.D. Chinn, Phys. Rev. Lett. 41 (1979) 955.
[9] J.S.C. Fain, M.D. Chinn and R.D. Diehl, Phys. Rev. B 21 (1980) 4170.
[10] S. Calisti, J. Suzanne and J.A. Venables, Surf. Sci. 115 (1982) 455.
[11] K. Kern, Phys. Rev. B 35 (1987) 8265.
[12] T. Aruga, H. Tochihara and Y. Murata, Phys. Rev. Lett. 52 (1984) 1794.
[13] C. Park, E. Bauer and H. Poppa, Surf. Sci. 187 (1987) 86.
[14] P.J. Feibelman, Phys. Rev. B 49 (1994) 14632.
[15] L. Pauling, The Nature of the Chemical Bond and the Structure of Molecules and Crystals (Cornell Univ. Press, Ithaca 1969)
[16] K. Jacobi and C.v. Muschwitz, Solid State Commun. 26 (1978) 477.
[17] D.W. Bullett, Surf. Sci. 102 (1981) L1.
[18] H. Brune, J. Wintterlin, J. Trost, G. Ertl, J. Wiechers and R.J. Behm, J. Chem. Phys. 99 (1993) 2128.
[19] J.-P. Lu, M.R. Albert and S.L. Bernasch, Surf. Sci. 258 (1991) 269.
[20] C.T. Campell and B.E. Koel, Surf. Sci. 183 (1987) 100.
[21] S.M. Davis and G.A. Somorjai, Surf. Sci. 91 (1980) 73.
[22] M. Poensgen, J.F. Wolf, J. Frohn, M. Giesen and H. Ibach, Surf. Sci. 274 (1992) 430.
[23] D.L. Doering and S. Semancik, Phys. Rev. Lett. 53 (1984) 66.
[24] C.R. Fuselier, J.C. Raich and N.S. Gillis, Surf. Sci. 92 (1980) 667.
[25] D.L. Doering, J. Vac. Sci. Technol. A 3 (1985) 809.
[26] J.P. McTague and A.D. Novaco, Phys. Rev. B 19 (1979) 5299.
[27] A.D. Novaco and J.P. McTague, Phys. Rev. Lett. 38 (1977) 1286.
[28] J. Wintterlin and R.J. Behm, Eds. H.J. Güntherodt and R. Wiesendanger (Springer, Berlin, 1992) p. 39.
[29] J. Flahaut, Ann. Chim. 7 (1952) 632.
[30] H. Hahn and G. Frank, Z. Anorg. Allg. Chem. 278 (1952) 333.
[31] C.R. Brundle, R.J. Behm and J. Barker, J. Vac. Sci. Technol. A 2 (1984) 1038.
[32] J.A. Wilson and A.D. Joffe, Adv. Phys. 18 (1969) 193.
[33] R. Coehoorn, C. Haas, J. Dijkstra, C.J.F. Flipse, R.A. de Groot and A. Wold, Phys. Rev. B 35 (1987) 6195.
[34] J.G. Forbes, A.J. Gellman, J.C. Dunphy and M. Salmeron, Surf. Sci. 279 (1992) 68.
[35] C.H. Patterson and R.M. Lambert, Surf. Sci. 187 (1987) 339.
[36] N.P. Prince, D.L. Seymour, M.J. Ashwin, C.F. McConville and D.P. Woodruff, Surf. Sci. 230 (1990) 13.
[37] L. Ruan, I. Stensgard, F. Besenbacher and E. Lægsgaard, Ultramicroscopy 42–44 (1992) 498.
[38] H.C. Galloway, J.J. Benítez and M. Salmeron, Surf. Sci. 298 (1993) 127.
[39] T.A. Land, T. Michely, R.J. Behm, J.C. Hemminger and G. Comsa, Surf. Sci. 264 (1992) 261.
[40] K.M. Ostyn and C.B. Carter, Surf. Sci. 121 (1982) 360.